

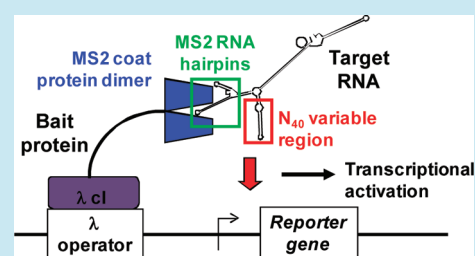
## Elucidation of Small RNAs That Activate Transcription in Bacteria

Michael S. Goodson,<sup>†</sup> John A. Lynch,<sup>‡</sup> Thomas Lamkin,<sup>§</sup> and Ryan Kramer<sup>\*,§</sup><sup>†</sup>711th Human Performance Wing, Air Force Research Laboratory, 2510 Fifth Street, Building 840, Wright-Patterson Air Force Base, Ohio 45433, United States<sup>‡</sup>Department of Chemistry, University of Cincinnati, Cincinnati, Ohio 45267, United States<sup>§</sup>711th Human Performance Wing, Air Force Research Laboratory, University of Cincinnati, 231 Albert Sabin Way, Medical Sciences Building, Cincinnati, Ohio 45221, United States

## Supporting Information

**ABSTRACT:** Small non-coding RNA (sRNA) control of gene expression has been shown to play a prominent role in genetic regulation. While the majority of identified bacterial sRNAs exert their control at the translational level, a few examples of bacterial sRNAs that inhibit transcription have also been identified. Using an engineered combinatorial RNA library, we have elucidated bacterial sRNAs that activate transcription of a target gene in *E. coli* to varying degrees. Mutation of the strongest activator modified its activation potential. Our results suggest that transcriptional activation of our target gene results from recruitment of the bacterial RNA polymerase complex to the promoter region. These data, coupled with the malleability of RNA, provide a context to define synthetic control of genes in bacteria at the transcriptional level.

**KEYWORDS:** small non-coding RNAs, transcriptional activation, bacteria, signal amplification, synthetic control



The central dogma of biology posits RNA as a conduit for genetic information to flow from DNA to proteins. However, the role of small non-coding RNA (sRNA) has been found to include a number of diverse biological functions, including the regulation of gene expression.<sup>1,2</sup> Indeed, sRNAs are hypothesized to be essential in the genomic programming of complex organisms.<sup>3</sup> The majority of identified bacterial sRNAs that regulate gene expression do so by either base pairing with other RNAs or binding and regulating protein activity.<sup>3,4</sup> Most of these interactions disrupt or modulate RNA translation. However, there is a growing class of bacterial sRNAs that are also known to inhibit transcriptional processes. These sRNAs act by binding to and inhibiting RNA polymerase<sup>5</sup> and by base pairing to mRNA to form a secondary structure that leads to transcriptional termination.<sup>6,7</sup> Activation of transcription by sRNA has been described in eukaryotes,<sup>8–10</sup> but no such activity has been implicated in bacterial gene regulation. Despite this, a number of sRNAs from a fragmented *E. coli* genome library have been found to bind to RNA polymerase with high affinity.<sup>11</sup> Thus, RNA-based regulatory elements may exist within the transcriptional processes of prokaryotes.

Synthetic biology aims to exploit cellular processes by genetically engineering key nodes in transcriptional and translational processes. The relative ease of engineering, screening, and modeling of RNA compared to that of proteins<sup>8,12,13</sup> uniquely identifies these biomolecules as highly engineerable elements for exploitation in synthetic systems. The most prominent methods for synthetic sRNA-based regulation of bacterial gene expression involve translational modulation via “riboswitches”,<sup>14–16</sup> binding and inhibition of a

specific bacterial transcription repressor,<sup>17</sup> or attenuating transcription through structural changes in RNA effected by antisense RNA.<sup>18</sup> Up-regulating transcription should increase reporter protein levels by orders of magnitude compared to translational control elements alone, where the amount of protein transcribed is dependent upon the number of transcripts available. This is particularly advantageous in engineered bacterial systems designed as cell-based reporters for environmental monitoring. The ability to exert both transcriptional and translational control within an engineered circuit also enables a number of different capabilities. For instance, redundancy in detection at both the transcriptional node and translational node could decrease false positives. Engineering different ligand detection schemes into each node also allows for more complex logic in biologically based detection and reporter systems.

Here we describe the first identification and characterization of bacterial sRNA transcriptional activators using an *in vivo* selection technique for prokaryotes and consequently add a new component to the tool kit of synthetic biology. A similar approach identified RNA-based transcriptional activators in yeast,<sup>8</sup> although the underlying mechanism was not elucidated. We show that the bacterial RNA transcriptional activators characterized here associate with the RNA polymerase complex of proteins and propose that the RNA initiates transcription through recruitment of the RNA polymerase holoenzyme.

Received: December 21, 2011

Published: March 15, 2012

## RESULTS AND DISCUSSION

**1. Identification of Potential RNA Transcriptional Activators.** In this study, we modified a commercially available bacterial two-hybrid system (BacterioMatch II two-hybrid system vector kit; Stratagene, La Jolla, CA) for the rapid selection of a RNA-based transcriptional activation sequence. Instead of monitoring protein–protein interaction via the assay, we exploited the high affinity interaction between the MS2 coat protein and the MS2 RNA hairpin. The bait plasmid (pBT) was modified by inserting the coding sequence for a MS2 coat protein dimer (Genescript, Piscataway, NJ) into the 3'-end of a  $\lambda$ CI coding sequence already present within the pBT plasmid. The resultant plasmid was termed pBT-MS2. The functional fusion protein  $\lambda$ CI-MS2 binds to the lambda operator located upstream of a *HIS3* reporter gene via the DNA binding domain of  $\lambda$ CI (Figure 1A). The commercial target vector (pTRG) was modified by replacing the coding region for the RNA

polymerase gene with a non-coding region that contained three distinct elements (Figure 1A). First, a RNA with a known stable secondary structure was included at the 5' and 3' ends to minimize transcript degradation.<sup>8</sup> Second, two MS2 RNA hairpins were included that localize the transcript to the promoter via interaction with the  $\lambda$ CI-MS2 fusion protein. Third, a variable library consisting of 40 randomly synthesized nucleotides was cloned upstream of the MS2 binding sequence. This element was screened for transcriptional activation at the reporter site. The resultant plasmid, containing all three components, was termed pTRG-var.

Both pBT-MS2 and pTRG-var. were cotransformed into *hisB* knockout *E. coli* containing an F' episome that included the reporter gene cassette. Growth of these bacteria on histidine-free minimal media supplemented with 3-amino-1,2,4-triazole (3-AT) was used as an indicator of *HIS3* transcriptional activation. 3-AT acts as a competitive inhibitor of the low levels of *HIS3* gene product produced by the reporter gene cassette even in the absence of transcriptional activation. As a result, the untransformed reporter strain was unable to grow on media lacking histidine in the presence of 3-AT. Similar approaches have been successfully utilized in previous yeast two-hybrid<sup>8</sup> and three-hybrid studies.<sup>19</sup>

Colonies were observed from cotransformations of pBT-MS2 and pTRG-var. plated onto 2 mM 3-AT selective screen plates. Compared to colonies grown on non-selective media, results indicated that ~0.1% of clones could grow on selective screen plates, a proportion similar to that found in a yeast model system.<sup>8</sup> A total of 22 positive cotransformations were identified, and all 22 grew on 3-AT selective screen plates after plasmid isolation and re-cotransformation. No colonies were observed from cotransformations of the unmodified pBT plasmid and a positive pTRG-var. This suggested that localization of the RNA transcriptional activator to the reporter gene is necessary for transcriptional activation. Similarly no colonies were observed from cotransformations of pBT-MS2 and pTRG that were plated onto selective screen plates. Alignment of the variable regions of the RNA constructs from these cotransformations exhibited large sequence variation without any obvious conserved domains, as evidenced by the long branch lengths and low bootstrap values in Figure 1B. Secondary structure analysis (mfold<sup>20</sup>) indicated that the variable regions of all the RNA transcriptional activators identified produced a structure in the RNA molecule that could be grouped into those producing a single, double, or paired stem-loop (Supplementary Figure S1). These data suggest that transcriptional control by sRNA is prevalent in bacteria, and that multiple biological interactions may drive transcriptional activation at the reporter site.

### 2. Selection of Strong Transcriptional Activators.

There was variation in the ability of the positive cotransformations to grow on plates containing increasing concentrations of 3-AT (Figure 2A). This suggested that there may be variation in the overall strength of transcriptional activation. To quantitatively address these variations, an initial selection procedure involving quantitative real-time PCR (QPCR) analysis and growth kinetics analysis (Supplementary Figure S2) was employed. Comparison of these methods identified statistically similar patterns of RNA transcriptional activation strength ( $\rho = 0.689$ ,  $P < 0.0005$ ). RNA transcriptional activators were categorized as “Strong”, “Medium”, or “Weak” based on comparing their ranks in the growth kinetics and the initial QPCR experiments. There was no obvious association

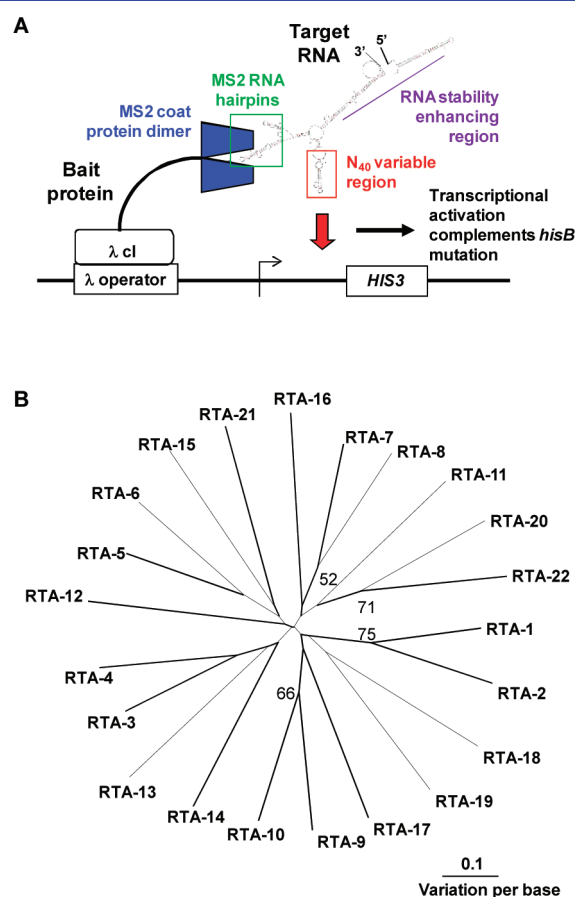


**Figure 1.** Screening for RNA transcriptional activation. (A) The bait plasmid carries  $\lambda$ CI genetically fused to a recombinant MS2 coat protein sequence that results in the translation of the fusion protein. The target plasmid contains three elements, an RPR region for transcript stability, a MS2 sequence that localizes the transcript to the  $\lambda$ CI-MS2 protein, and a N40 variable region. The sequence contains no translational signals and is maintained intracellularly as an RNA transcript. Only those RNA library members that activate transcription of *HIS3* allow survival on selective screen media. (B) Unrooted phylogenetic tree produced by the neighbor-joining method, using Kimura two-parameter distances between the variable regions of RNA molecules that could activate transcription of *HIS3*. Gapped positions were included in the analysis. Percentage bootstrap values >50 are indicated. See also Supplementary Figure S1.

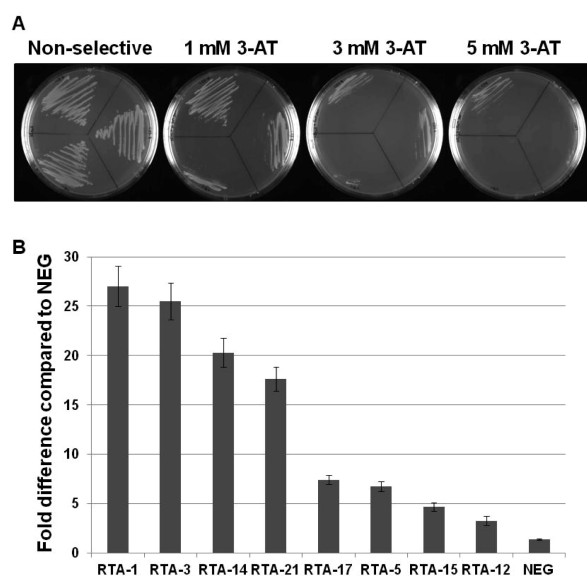


**Figure 2.** Assessment of the strength of transcriptional activation. (A) Variation in the strength of transcriptional activation as determined by the ability to grow on increasing concentrations of 3-AT. Strains were streaked onto plates and incubated at 37 °C for 24 h. Upper segment, RTA-3; right-hand segment, RTA-5; lower segment, RTA-12. (B) Average fold difference of *HIS3* expression normalized to RNA transcriptional activator expression of “Strong”, “Medium”, and “Weak” transcriptional activators compared to NEG. Fold difference was compared using the  $\Delta\Delta\text{Ct}$  method. Each individual Ct value of three replicates of three biological replicates per transcriptional activator were compared to the mean NEG Ct to calculate each  $\Delta\Delta\text{Ct}$  value ( $n = 81$ ). Data are represented as mean  $\pm$  SEM.

between strength of activation and predicted secondary structure. Representatives of the Strong, Medium, and Weak RNA transcriptional activators were used in two additional biological replicates of the QPCR analysis. For all QPCR experiments, a low variation in Ct value was observed within each triplicated sample. Strong RNA transcriptional activators had consistently higher fold differences than Medium and Weak RNA transcriptional activators. There is a significant difference in activation strength among the Strong RNA transcriptional activators (ANOVA,  $P < 0.0005$ ) (Figure 2B). The two strongest RNA transcriptional activators, RTA-1 and RTA-3, are significantly different from RTA-21 (Tukey’s pairwise comparison,  $P < 0.01$ ). There is no significant difference between RTA-1 and RTA-3 ( $t$  test,  $P > 0.2$ ). As a further selection procedure, the growth of each of the four strongest RNA transcriptional activators was assessed on 5 mM and 3 mM 3-AT selective screen plates (Table 1). These concentrations of 3-AT were more stringent than for the initial screening of pBT-MS2 and pTRG-var. cotransformants. Selectivity was confirmed by the growth of the positive control cotransformed *E. coli* (pBT-LGF2 pTRG-Gal11<sup>P</sup>) on all of the selection plates after 18 h (Table 1), while the negative control cotransformed *E. coli* grew only on the non-selective screen plates. Three of the four strong RNA transcriptional activators, RTA-3, RTA-14, and RTA-21, grew on the most stringent (5 mM 3-AT) selective screening plate after 24 h. However, of these three, RTA-21 grew only slowly, as evidenced by the formation of small colonies. These three strong RNA transcriptional activators exhibited colony growth on the 3 mM selective screen after 24 h incubation, although the colonies from RTA-21 were small. RTA-1 exhibited colony

**Table 1.** Assessment of Growth of the Strongest RNA Transcriptional Activators on Plates of Differing Selection Stringency<sup>a</sup>

sample	5 mM 3-AT			3 mM 3-AT			no 3-AT		
	18 h	24 h	32 h	18 h	24 h	32 h	18 h	24 h	32 h
RTA-3	×	++	++	×	++	++	++	++	++
RTA-1	×	×	×	×	×	+	++	++	++
RTA-14	×	++	++	×	++	++	++	++	++
RTA-21	×	+	+	×	+	+	++	++	++
positive	++	++	++	++	++	++	++	++	++
negative	×	×	×	×	×	×	++	++	++

<sup>a</sup>× = no colonies; + = small colonies; ++ = large colonies.

growth on the 3 mM selection plates after 32 h incubation. All samples grew on the non-selective screen after 18 h of incubation.

In order to determine the strongest RNA transcriptional activator, their order in the growth kinetics analysis, the compiled real-time PCR data, and results from the selective screen assay were converted to a rank. For the latter, rank was attributed using qualitative growth rates on the 5 mM 3-AT selective screen. Using this criteria, the strongest RNA transcriptional activator was determined to be RTA-3 (Table 2). This RNA had no similarity to sequences present in the *E.*

**Table 2.** Selection of the Strongest RNA Transcriptional Activator

sample	rank			total
	growth rate constant, $k$ (Supplementary Figure S2)	compiled QPCR (Figure 2C)	selective screen assay (Table 1)	
RTA-3	1	2	1	4
RTA-1	2	1	4	7
RTA-14	4	3	1	8
RTA-21	3	4	3	10

*coli* genome (BLAST<sup>21</sup>). RTA-3 was subsequently used in mutational studies aimed at determining sequence relevancy and analyses to determine the possible interacting proteins that drive transcriptional activation.

**3. Identification of Interacting Proteins.** To investigate which proteins potentially interact with the RNA transcriptional activator, an electrophoretic mobility shift and protein sequencing assay was employed. A biotinylated, RNA probe to the conserved 3’ end of RTA-3 was used to qualitatively determine if the RNA transcriptional activator interacted with native *E. coli* proteins. Mobility shifts of the biotinylated RNA probe were seen in native gel electrophoresis of cotransformed RTA-3 bacterial cell extract (Supplementary Figure S3). Sequencing of the regions of gel showing a probe size shift returned a total of 37, 61, and 89 proteins with significant ( $P < 0.005$ ) matches to the NCBI database, for regions 1, 2, and 3, respectively (Supplementary Table S1). Three members of the RNA polymerase holoenzyme were abundant in regions 1 and 2. RNA polymerase beta (*rpoB*) was the second and third most abundant protein in regions 1 and 2, respectively. RNA polymerase sigma 70 (*rpoD*) was the 12th most abundant protein in region 1, and RNA polymerase alpha (*rpoA*) was the 17th and 15th most abundant protein in regions 1 and 2, respectively. The *rpoB* catalyzes the synthesis of RNA, while

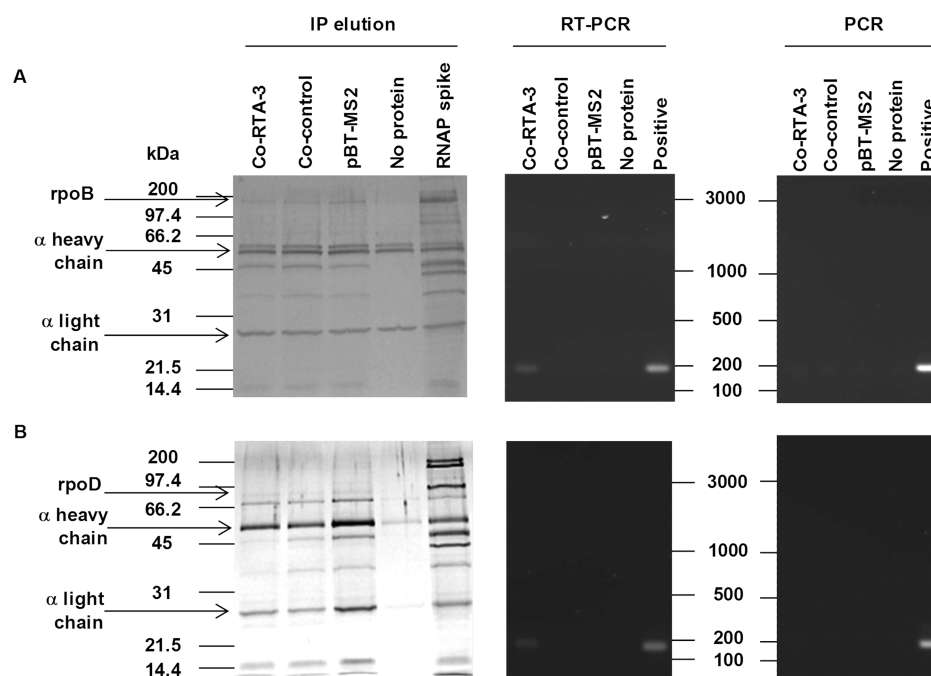


**Figure 3.** Immunoprecipitation of RTA-3 with rpoB and rpoD. Reverse transcription PCR and PCR of the eluate from the rpoB immunoprecipitation (A) and the rpoD immunoprecipitation (B) using RNA transcriptional activator-specific primers. Amplicon sizes of 193 bp and 163 bp are expected for RTA-3 and control, respectively. No DNA contamination of the eluate by the target plasmid was detected. No Protein, control immunoprecipitation experiment performed without the addition of cell lysate; RNA spike, lysate from co-RTA-3 culture spiked with RNA polymerase holoenzyme; Positive, reactions performed with purified pTRG-RTA-3 as the template. Gels are representative of three independent experiments.

rpoA assembles the enzyme and binds regulatory factors. The rpoD is required to enable specific binding of RNA polymerase to the promoters of most genes required in growing cells.<sup>22</sup> The lambda repressor protein  $\lambda$ cI was identified in region 3, suggesting that the interaction between bait and target complex remained intact under native electrophoresis. These analyses suggested that our identified transcriptional activator RTA-3 may recruit the polymerase complex to the reporter gene promoter region.

To test this conclusion, we investigated whether the RNA transcriptional activator could be co-immunoprecipitated with RNA polymerase subunits using antibodies to rpoB and rpoD. To account for non-specific RNA binding, immunoprecipitation experiments included cell extracts from bacteria transformed with pBT-MS2 and a target plasmid that was unable to activate transcription, pTRG-control. This target plasmid was identical to pTRG-var. except that it contained a 10-nucleotide insert instead of the 40-nucleotide variable region. As expected, each subunit was immunoprecipitated from cell lysates of bacteria cotransformed with pBT-MS2 and pTRG-RTA-3, as well as bacteria cotransformed with pBT-MS2 and pTRG-control, and transformed with pBT-MS2 alone. Reverse transcription PCR (RT-PCR) was performed using primers specific to the transcriptional activator to identify if RTA-3 was co-precipitated with rpoB and rpoD. The RNA transcriptional activator RTA-3 was detected in the rpoB and rpoD precipitated fraction from bacteria cotransformed with the bait plasmid and pTRG-RTA-3 (Figure 3). No RT-PCR product was seen in the rpoB and rpoD precipitated fraction from bacteria cotransformed with the bait and pTRG-control plasmid or the bait plasmid alone. PCR analysis determined that there was no bait or target plasmid DNA contamination of the eluate that may have given rise to a false positive (Figure 3). Taken together, these results

indicate that the RTA-3 RNA transcript was able to be co-immunoprecipitated with the RNA polymerase subunits, rpoB and rpoD. Direct or indirect recruitment of RNA polymerase to the promoter region of the reporter by the RNA transcriptional activator would have the direct effect of stimulating or enhancing transcription from this site.

**4. Mutagenesis of the Strongest RNA Transcriptional Activator.** The sequence variability exhibited in the identification of potential RNA transcriptional activators in our initial screen and the differences in their strength of activation suggest that modification of a specific RNA transcriptional activator will affect its activation capability. To test this hypothesis we investigated the effect of randomly mutating the 40-nucleotide insert region of the strongest transcriptional activator, RTA-3, to determine if the strength of transcriptional activation could be changed and to elucidate which parts of this region were essential for activation. The resultant clones were subjected to the selection procedures described above. An average of 4.9 (SE = 0.5) mutations per clone was achieved. Twenty-six mutagenized variants of RTA-3 were able to grow on 3-AT selective screen media. The consensus sequence of the aligned mutations (Figure 4A) was identical to the variable region of RTA-3, suggesting that RTA-3 is already relatively well optimized in its ability to activate transcription. However, there was only one conserved residue in all of the mutant clones (A30) that closed a loop near the end of the single stem predicted to form in RTA-3. Thirteen additional columns showed one or more substitutions of the same nucleotide, including a region of six consecutive bases (19–24). This region corresponds to the terminal loop of the single stem formed by RTA-3 (Supplementary Figure S1). To assess the strength of activation, QPCR was performed as described above except that fold difference was expressed relative to the level of

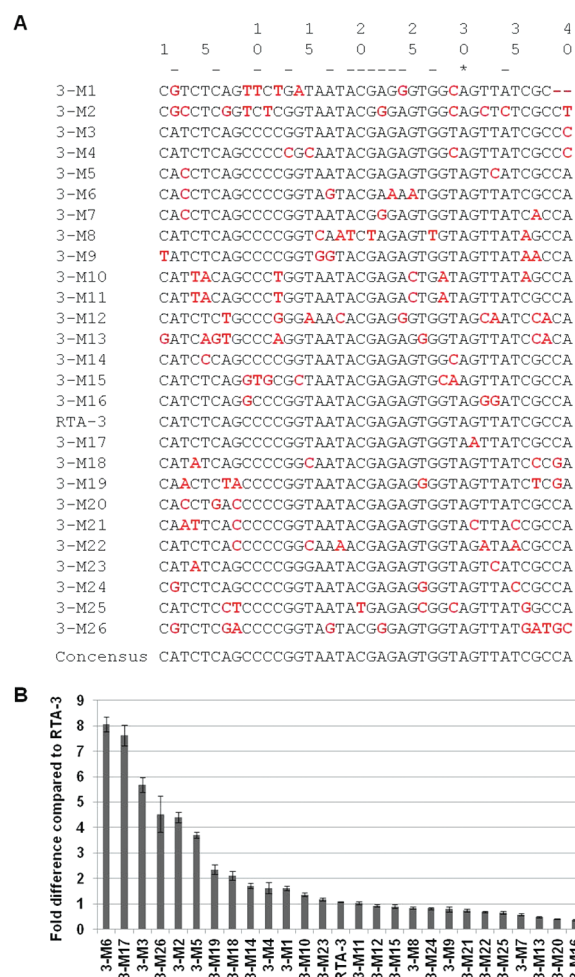


**Figure 4.** Evolution of stronger activators. (A) Alignment of mutated RTA-3 sequences that grow on 3-AT selective screen media. Stars indicate conserved nucleotides. Dashes indicate columns that have one or more substitutions of the same nucleotide. Mutations are highlighted in red. (B) Average fold difference of *HIS3* expression normalized to RNA transcriptional activator expression compared to RTA-3. Fold difference was compared using the  $\Delta\Delta C_t$  method. Each individual  $C_t$  value of three replicates of three biological replicates per mutant were compared to the mean RTA-3  $C_t$  to calculate each  $\Delta\Delta C_t$  value ( $n = 81$ ). Data are represented as mean  $\pm$  SEM. See also Supplementary Figure S4.

transcriptional activation exhibited by RTA-3 (Figure 4B). Six mutants exhibited a greater than 3-fold increase in transcriptional activation compared with that of RTA-3, with the strongest activator, 3-M6, exhibiting an 8-fold increase. This is comparable to a similar study performed in yeast,<sup>8</sup> although we found less sequence conservation between mutants than in that study. Two mutant clones, 3-M6 and 3-M17, are significantly stronger transcriptional activators than the others (ANOVA;  $P < 0.0001$ ), although they are not significantly different from each other ( $t$  test;  $P > 0.1$ ). Interestingly, two of the three strongest transcriptional activators, 3-M17 and 3-M3, differed from RTA-3 by only a single base. There was no obvious effect of secondary structure on activation strength, although *mfold* predictions of the mutated activators showed that the two mutant clones exhibiting the strongest transcriptional activation, 3-M6 and 3-M17, had a similar triple stem-loop structure despite their sequence differences (Supplementary Figure S4). However, the only other mutant clone predicted to have a

similar triple stem-loop structure, 3-M21, exhibited transcriptional activation weaker than that of the original RTA-3 clone. The semiconserved consecutive nucleotides 19–24 of the 40-nucleotide insert formed the terminal loop of the middle stem in all three clones. However, the length of the predicted stems in 3-M21 were shorter than those of 3-M6 and 3-M17. The mutant clones exhibiting the weakest transcriptional activation compared to the original RTA-3 clone, 3-M13, 3-M20, and 3-M16, had 8, 3, and 3 substitutions, respectively. Similarly, there was no obvious difference in their predicted secondary structure compared to clones that had a transcriptional activation capability higher than that of RTA-3 (Supplementary Figure S4). These data suggest that both sequence and structure are important determinants of activation strength. This, coupled with the requirement for localization of the RNA transcriptional activators upstream of the reporter gene in our system, supports the recruitment model of transcriptional activation<sup>22</sup> in bacteria.

RNA molecules share many chemical features found in protein transcriptional activators,<sup>8</sup> and these features may be sufficient to allow non-natural RNA sequences to interact with RNA polymerases to mediate transcription. Our experiments show that the RTA-3 RNA transcriptional activator does associate with the bacterial RNA polymerase complex, and it is likely that recruitment of the RNA polymerase by the activator is sufficient to activate transcription of the adjacent reporter gene, in line with the recruitment model of transcriptional activation. Protein-based, natural bacterial transcriptional activators have been shown to bind to different parts of the RNA polymerase holoenzyme to activate transcription.<sup>22–24</sup> While we have not been able to identify which part of the bacterial RNA complex our strongest RNA transcription activator associates with, the recruitment model suggests that a specific interaction or recognition site is not a requirement of activation. It is not inconceivable to suggest that the RNA transcriptional activator may interact with multiple parts of the RNA polymerase complex. Indeed, the variation in strength of activation may be associated with the number of contact sites between the activator and polymerase,<sup>22</sup> with increased contact sites increasing the activation strength, potentially through higher binding leading to increased “ON” time for the polymerase in this stochastic system. The variation in strength of activation of the mutated RTA-3 activator suggests that even small changes in sequence and subtle changes in secondary structure can affect the activation strength, possibly by affecting interactions with the RNA polymerase complex.

By selecting for sequences that activate transcription from a random RNA library and then mutagenizing the strongest activator to change its activation strength, we have increased the repertoire of building blocks for use in synthetic biology. These RNA molecules perform “protein-like” functions, without the difficulty and *in vivo* immunogenic limitations of proteins.<sup>10</sup> In the same way that the modular components of eukaryotic transcription factors can aid in the synthesis of genetic switches,<sup>22</sup> coupling two RNA building blocks consisting of an aptamer specific to a molecule of interest and a RNA transcriptional activator would allow controlled regulation of transcription. RNA-based ligand-dependent transcriptional activation has been shown to be achievable in yeast,<sup>25</sup> and our findings suggest that a sRNA with a similar function can be engineered in bacteria.

## METHODS

All chemicals were purchased from Sigma-Aldrich, and all restriction enzymes were purchased from NEB, unless otherwise stated. All media was prepared as described in the BacterioMatch II 2-hybrid system vector kit protocol (Stratagene).

**1. Synthesis of the Target and Bait Vectors.** The commercial target vector pTRG from the BacterioMatch II two-hybrid system vector kit (Stratagene) was modified by adding a MfeI restriction site upstream of the pTRG promoters *lpp* and *lac-UV5* (pTRG-MfeI) using the QuikChange kit (QIAGEN). This allowed a synthesized stretch of DNA consisting of an MfeI restriction site, the promoters *lpp* and *lac-UV5*, a RNase P leader, *Bam*HI and *Not*I restriction sites, MS2 hairpins, a RNase P terminator, and a *Xho*I restriction site (GenScript) to be inserted in place of the pTRG RNA polymerase alpha gene. Briefly, the synthesized DNA and pTRG-MfeI were double digested using MfeI and *Xho*I, and digested products of the expected size were gel purified using QIAquick spin minicolumns (QIAGEN) and ligated using T4 DNA ligase (3 U/mL; Promega). Ligation products, uncut pTRG (positive control), and gel-excised, double digested pTRG alone (negative control) were transformed into *E. coli* XL1 Blue MRF' Kan competent cells by heat shock following the protocol described by the BacterioMatch II manual (Stratagene). Transformation mixtures were plated onto LB-tetracycline selection plates. Insertion of the synthesized DNA was confirmed by PCR, restriction digest, and sequencing of plasmids purified from transformed colonies. Sequencing was performed by Genewiz. Sequences were aligned using ClustalX.<sup>26</sup> This modified target vector is henceforth referred to as pTRG-MS2.

A blunt-ended double-stranded variable library was synthesized from a 70 -nucleotide primer (Integrated DNA Technologies) containing a 40-nucleotide variable sequence between *Bam*HI and *Not*I restriction sites, using a specific reverse primer and the Klenow fragment of *E. coli* DNA polymerase I (NEB). A variable region of 40 nucleotides was chosen since results from previous studies in yeast<sup>8,9</sup> suggested that this length encouraged secondary structure formation while balancing the instability of longer RNA sequences with the presence of degradation-prone unstructured single-stranded regions in shorter lengths. The variable library and the modified commercial target vector, pTRG-MS2, were double digested using *Bam*HI and *Not*I. Products were gel purified using the QIAEX II system (QIAGEN) and ligated using T4 DNA ligase (Promega). Ligations were transformed in duplicate into XL1-Blue MRF' Kan strain *E. coli* by the heat shock technique. The resultant transformation culture was plated onto LB-tetracycline selection plates. Transformation using an uncut pTRG plasmid and a ligation reaction containing no plasmid were performed as positive and negative controls, respectively. Insertion of the variable library was confirmed as described above. No similarity was exhibited by 25 clones sequenced to assess library diversity. This modified target vector is henceforth referred to as pTRG-var.

The commercial bait vector, pBT, was modified by inserting a synthesized stretch of DNA encoding a MS2 coat protein dimer, terminating with *Not*I and *Xho*I restriction sites (GenScript) into the multiple cloning site. Digested products of the expected size were gel purified using QIAquick spin minicolumns (QIAGEN) and ligated using T4 DNA ligase (3 U/

mL; Promega). Ligation products, uncut pBT (positive control), and gel-excised double digested pBT alone (negative control) were transformed into *E. coli* XL1 Blue MRF' Kan competent cells by the heat shock technique. Transformation mixtures were plated onto LB-chloramphenicol selection plates. Insertion of the variable library was confirmed by as described above. This modified bait vector is henceforth referred to as pBT-MS2.

**2. Expression of pTRG-var. and pBT-MS2.** Expression of the inserted DNA in the pTRG-var. plasmid can be induced by IPTG. RNA expression was confirmed by growing *E. coli* XL1-Blue MRF' cells transformed with pTRG-var. in LB tetracycline + IPTG at 30 °C, extracting RNA, and detecting presence of the transcript by reverse transcription-PCR (RT-PCR). RNA was extracted using the MasterPure Complete DNA and RNA Purification Kit (Epicenter Biotechnologies), following the manufacturer's protocol for cell samples, except that double the suggested amount of DNase I was used. RT-PCR was carried out using primers (RTRNA-F, GGCTAGAACTAGTG-GATCC,  $T_m$  51.5 °C and RTRNA-R, TTGGATATGGGG-GAATTCC,  $T_m$  51.7 °C) that anneal to regions within the insert using the Access RT-PCR System (Promega). Reactions were carried out using 20–50 ng total RNA and an amplification annealing temperature of 51 °C. Results were analyzed by gel electrophoresis. No DNA contamination was detected using reactions without reverse transcriptase.

IPTG induction of pBT-MS2 should result in expression of a protein encompassing both the  $\lambda$ CI and the MS2 coat protein dimer. Protein expression was confirmed by growing *E. coli* XL1-Blue MRF' cells transformed with pBT+MS2 in M9+ His-dropout broth + chloramphenicol and IPTG, extracting protein and performing a Western blot using an antibody to the  $\lambda$ CI protein (Stratagene). Protein was extracted using the BugBuster protein extraction reagent (EMD Biosciences), following the manufacturer's protocol. Soluble protein quantities were assessed using the BCA protein assay (Thermo Fisher Scientific) using a Nanodrop spectrophotometer (Thermo Fisher Scientific). SDS-PAGE and Western blots were performed using the NuPAGE Novex Bis-Tris gels, the XCell Surelock Mini Cell electrophoresis apparatus, and the XCell II Blot module (Invitrogen). Cross-reactive bands were detected using the ECL plus Western blotting detection system (Amersham- GE Healthcare), following the manufacturers protocol, and photographic film and developer (Kodak).

**3. Identification of Potential RNA Transcriptional Activators.** Cotransformation was performed by following the BacterioMatch II two-hybrid system vector kit protocol (Stratagene). Briefly, BacterioMatch II validation reporter competent cells were cotransformed by heat shock with the bait and target vector, and plated onto non-selective screening plates and 2 mM amino-1,2,4-triazole (3-AT) selective screening plates. Cotransformation was performed using 50 ng pTRG-var. and pBT-MS2, and also 50 ng positive control target (pTRG\_Gal11<sup>P</sup>) and bait (pBT\_LGF2) vectors supplied with the BacterioMatch II kit. Additionally transformations using 50 ng pBT-MS2 alone, and a no vector control were also performed. The number of colonies on each plate was assessed after incubation at 37 °C for 24 h. An additional 24 h incubation was performed in the dark at room temperature to allow growth of cells harboring weak interactors and/or expressing proteins that may be toxic to the cells. As expected, the proteins expressed by the positive control bait and target plasmids interact strongly and therefore a similar number of

colonies ( $10^4$ – $10^5$  cfu per plate) were visible on the non-selective and selective screening plates. The pTRG-var. pBT-MS2 cotransformation had a transformation efficiency of  $\sim 10^6$  cells/mg, based on growth on non-selective screening plates. The “no vector” control and the bait vector alone produced no colonies on the non-selective or selective screening plates. Colonies were screened on 54 selective screening plates. The average number of cotransformed colonies counted on non-selective screening plates was  $7 \times 10^3$ , suggesting that potentially  $4 \times 10^5$  clones were finally screened. Colonies that grew on selective screen plates were further verified by performing re-cotransformation of pBT-MS2 and the pTRG-var. vector isolated from the original potential positive clone. Plates were incubated at 37 °C for 24 h followed by incubation at room temperature in the dark for 24 h. Verified positives were sequenced in both directions and analyzed as described above. A bootstrapped (1,000 iterations) neighbor-joining tree of the positive sequences was constructed based on the Kimura two-parameter correction using ClustalX,<sup>26</sup> with gapped positions included.

**4. Selection of Strong Transcriptional Activators.** A total of 22 positive cotransformations were identified. The relative strengths of activation of these positives were assessed using growth kinetics analysis and quantitative real-time PCR (QPCR). Assessing the growth rate of the positive clones in 3-AT selective media is an indirect way of measuring transcription of the *HIS3* gene. Higher growth rates will correspond to an increased ability to synthesize histidine and therefore an increased ability to grow on selective media. The BacterioMatch II positive cotransformation described above provided a positive control. A pBT-MS2 and pTRG-var. cotransformation that was picked from a non-selective screen plate and did not grow after incubation on a 2 mM selective screen plate was used as the negative control in these analyses. Glycerol stocks of each transcriptional activator and control cotransformation were streaked onto non-selective screen plates. These plates were incubated at 37 °C for 24 h. A single colony from each cotransformation was used to inoculate 2 mL of non-selective screen media and the inoculated cultures were incubated overnight at 37 °C with shaking at 215 rpm. For each sample, 10  $\mu$ L of overnight culture was added to 150  $\mu$ L of 2 mM 3-AT selective screen media in the wells of a 96-well plate. Each sample was prepared in triplicate. The plate was incubated at 37 °C with shaking and the absorbance at 600 nm ( $A_{600}$ ) of each well was read every 20 min for 8 h using a programmable plate reader (Synergy 2; BioTek). Growth curves of  $\log(A_{600})$  against time were produced, and the mean growth rate constant,  $k$ , was calculated during logarithmic growth of each sample using the following equation:

$$k = \frac{\log(A_{600})_{t_1} - \log(A_{600})_{t_0}}{0.301t}$$

QPCR allows direct measurement of *HIS3* transcription relative to the amount of RNA transcriptional activator present. The negative control cotransformation was the same as described for the growth curve analysis. No positive control cotransformation was available since the normalizing RNA is the RNA transcriptional activator that was inserted into the target plasmid, which is absent from the BacterioMatch II kit positive control cotransformations. Glycerol stocks of each transcriptional activator and control cotransformation were streaked onto non-selective screen plates. These plates were incubated at 37 °C for 24 h. A single colony from each

cotransformation was used to inoculate 2 mL of non-selective screen media, and the inoculated cultures were incubated overnight at 37 °C with shaking at 215 rpm. For each positive and control, 50  $\mu$ L of overnight culture was added to 2 mL of 1 mM 3-AT selective screen media and incubated at 37 °C with shaking at 215 rpm for 3 h. RNA was extracted from each culture as described above. RT-PCR reactions with reverse transcriptase omitted were used to confirm that there was no DNA contamination of the RNA isolations. Quantity and quality of RNA was determined by absorbance (Nanodrop spectrophotometer; Thermo Fisher Scientific) and gel electrophoresis, respectively. One microliter of total RNA was made into cDNA using the iScript select cDNA synthesis kit (Bio-Rad) following the manufacturer's protocol for random hexamer primed reactions. QPCR was performed using an ABI 7500 Fast real-time PCR machine in association with primers and probes designed using the Custom TaqMan gene expression assay service utilizing the TaqMan chemistry real-time PCR protocol (Applied Biosystems). Primers and FAM-labeled probes were designed to specifically recognize the cDNA sequences of *HIS3* (*HIS3F*, TGCTCTCGGTCAAGCTTTTAAAGA; *HIS3R*, CGCAATCCTGATCCAAACCTTTT; *HIS3FAM*, CACG-CACGGCCCCCTAG) and the RNA transcriptional regulator (*varRNAF*, GCGGCTGGGAACGAAAC; *varRNAR*, CCAC-TAGTTCTAGCCGGAATTCTG; *varRNAFAM*, CCAATCG-CAGTCCCA). Briefly, QPCR reactions were set up using 10  $\mu$ L of 2x TaqMan Fast universal PCR Mastermix (Applied Biosystems), 1  $\mu$ L of 20x TaqMan gene expression assay mix containing the primers and probe for either *HIS3* or the RNA transcriptional activator, 1  $\mu$ L of cDNA, and 8  $\mu$ L nuclease-free water per sample. Ten-fold serial dilutions of a representative cDNA sample were also prepared to assess the efficiency of the reaction for each gene of interest. Samples were prepared in triplicate and loaded into a 96-well plate. Reactions were run using the following thermal profile: 95 °C for 20s; 40 cycles of 95 °C for 3s, 60 °C for 30s. Wells were analyzed during the anneal/extension step. Samples were analyzed using the ABI 7500 Fast system software utilizing the  $\Delta\Delta C_t$  method of relative quantification.<sup>27</sup> The relative fold difference of *HIS3* expression of each sample compared to the negative was normalized using RNA transcriptional activator expression. This method assumes optimum efficiency of each reaction. Reaction efficiency was calculated using the following equation:

$$\text{efficiency} = 10^{(-1/\text{slope})}$$

where slope is the slope of a graph of Ct value against  $\log(\text{dilution})$ . An efficiency of 2 is considered optimal since it indicates that the amplicon concentration is doubling with every amplification cycle. Average reaction efficiency was 2.020 (SE = 0.018). Correlation of the results of the growth curve analysis and the QPCR analysis was tested using a Spearman's rank correlation coefficient test. The Spearman's rank coefficient,  $\rho$ , varies from 1 (perfect agreement between two rank orders) through 0 (rankings are completely independent) to  $-1$  (one ranking is the reverse of the other). Confidence levels can be applied to  $\rho$  using published  $\rho$  statistical tables. Growth curve analysis and QPCR analysis gave statistically similar results (Spearman's Rank Correlation coefficient,  $\rho$ , of 0.689,  $P < 0.0005$ ).

RNA was extracted from representative samples deemed to be Strong, Medium, or Weak transcriptional activators. Two

RNA extractions were performed for each sample, each grown from a separate cfu from a streak of the glycerol stock of that sample. RNA extractions and QPCR analyses were performed as described above. Average reaction efficiency was 2.022 (SE = 0.014). In addition to comparing within each biological replicate, each individual Ct for HIS and VAR of the three biological replicates of each sample were compared to the mean of the NEG Ct to calculate the  $\Delta\Delta\text{Ct}$  value. Thus there is a fold difference value for each combination of HIS Ct ( $n = 9$ ) to VAR Ct ( $n = 9$ ), and therefore  $n = 81$  for each RNA transcriptional activator. The means of the pooled fold difference values for each RNA transcriptional activator were compared by a one-way analysis of variance followed by Tukey's pairwise comparison (95% confidence interval). Individual pairs of data were compared by  $t$  test.

To verify that the four strong RNA transcriptional activators determined in the above experiments were true positives, their growth was determined on stringent 3-AT selective screen plates. Glycerol stocks of each positive and control cotransformation were used to inoculate 1.5 mL tubes containing 750  $\mu\text{L}$  of non-selective screen media. The inoculated cultures were incubated at 37 °C for 30 min. One hundred microliters of each culture was plated onto either 5 mM 3-AT selective screen plates, 3 mM 3-AT selective screen plates, or non-selective screen plates. These plates were incubated at 37 °C. Growth was assessed by visualizing the plates after 18, 24, and 32 h. In order to identify the strongest RNA transcriptional activator, their order in the growth kinetics assay and the compiled real-time PCR data was converted to a rank (with highest mean fold difference assigned to a rank of 1), as was their order in the selective screen assay. For the latter, rank was attributed to the rapidity of growth on the 5 mM 3-AT selective screen, with the fastest growth assigned a rank of 1.

### 5. Identification of Interacting Proteins by EMSA.

Stabs from glycerol stocks of each sample and control cotransformation were used to inoculate 2 mL of non-selective screen media. However, the untransformed BacterioMatch II screening reporter strain competent cells were grown in M9+ HIS-dropout broth alone, and the pBT-MS2 alone transformation was grown in M9+ HIS-dropout broth + 25  $\mu\text{g}/\text{mL}$  chloramphenicol. The inoculated cultures were incubated overnight at 37 °C with shaking at 215 rpm. For each sample and control, 1 mL of overnight culture was added to 100 mL of their respective growth media and incubated overnight at 37 °C with shaking at 215 rpm. Total soluble proteins were extracted as described above. Soluble protein quantities were assessed using the BCA protein assay (Thermo Fisher Scientific) and a Nanodrop spectrophotometer (Thermo Fisher Scientific).

EMSA were performed in triplicate using the LightShift Chemiluminescent EMSA kit (Pierce) following the manufacturer's protocol. A biotinylated RNA probe (5'BioVar266-288, Biotin-GAAGUUGGAUAUGGG) was synthesized (Integrated DNA Technologies) that would complement the conserved 3' end of the RNA transcriptional activator at nucleotides 266–288. Reaction conditions were optimized using the LightShift EMSA optimization and control kit, and RNase inhibitor was added to each binding reaction. The optimized binding conditions for probe 5'BioVar266–288 were as follows: 1X Binding Buffer; 50 ng/mL Poly (dI dC), 1 U/mL Superase-In (Ambion), 50 nM biotinylated probe, 2.5% glycerol, 5 mM  $\text{MgCl}_2$ , 0.05% NP-40, 10 mM EDTA, and 100  $\mu\text{g}$  soluble protein extraction. These conditions were used in all

proceeding experiments. To investigate the specificity of binding, binding reactions were performed using the optimized probe conditions described above with and without a 100-fold excess of unbiotinylated probe. Native gel electrophoresis was performed using the NativePAGE Novex Bis-Tris gel system (Invitrogen). Duplicate gels were run. One of the gels was Coomassie stained. The duplicate native gel was transferred onto a nylon membrane, protein was cross-linked to the membrane by UV irradiation, and the probe was detected using the Chemiluminescent Nucleic Acid Detection Module. Bands of interest were matched to identical regions of the Coomassie stained gel, which were excised and sequenced by mass spectrometry analysis (Cancer and Cell Biology Proteomics Core Facility, University of Cincinnati).

**6. Immunoprecipitation of RNA Transcriptional Activator Using RNA Polymerase Subunits.** Immunoprecipitation experiments were devised to investigate if the RNA transcriptional activator could be isolated using antibodies to rpoB and rpoD, two RNA polymerase subunits protein identified in the EMSA sequencing. The immunoprecipitation and analysis was carried using the Classic IP kit (Pierce) following the manufacturer's protocol, using the low-pH elution method to avoid denaturing conditions associated with the sample-buffer elution method. Briefly, the antibody is incubated with cell lysate to form an immune complex. The immune complex is captured using Protein A/G linked agarose beads in a minicolumn. After washing, the antibody-immune complex is eluted. The first wash and the elution was run on a SDS-PAGE gel and visualized using the SilverQuest staining kit (Invitrogen) and also used as template for PCR and reverse-transcriptase PCR using RTA-specific primers as described above. The control target plasmid, pTRG-control, was constructed as described for pTRG-var., except that a 10-nucleotide region that complemented the sequence opposite to the base of the stem-loop formed by the variable region in pTRG-var. (TCTAGAGTCG) replaced the 40-nucleotide variable region. *E. coli* cotransformed with pBT-MS2 and pTRG-control were not able to grow on 1 mM 3-AT. To facilitate identification of immunoprecipitated RNA polymerase subunits, cell lysate from a co-RTA-3 culture was also spiked with 5 U of *E. coli* RNA polymerase holoenzyme (Epicenter) before performing the immunoprecipitation.

**7. Mutagenesis of the Strongest Transcriptional Activator.** The RTA-3 clone was mutated using the JBS dNTP-mutagenesis kit (Jena Bioscience) following the manufacturer's protocol. Briefly, RTA-3 was amplified from pTRG-RTA-3 in the presence of dNTPs and mutagenic dNTP analogues 8-oxo-dGTP and dPTP using primers RTRNA-F and RanMut-R (GCAGGCATGCGCGGCCGC,  $T_m$  69.4 °C). Thirty PCR cycles were run to maximize the rate of mutagenesis. The mutagenic dNTP analogues are eliminated from the resultant amplicon by subjecting it to a second PCR containing natural dNTPs. Cloning, screening for transcriptional activation, and sequence identification of the mutants were performed as described above.

QPCR was used to determine the strength of transcriptional activation of the RTA-3 mutants. Briefly, RNA was extracted from clone RTA-3 and the RTA-3 mutant transcriptional activators. Three RNA extractions were performed for each sample, each grown from a separate cfu from a streak of the glycerol stock of that sample. RNA extractions and QPCR analyses were performed as described above. Average reaction efficiency was 2.015 (SE = 0.014). Each individual Ct for HIS



and VAR of the three biological replicates of each sample were compared to the mean of the RTA-3 Ct to calculate the  $\Delta\Delta\text{Ct}$  value. Thus there is a fold difference value for each combination of HIS Ct ( $n = 9$ ) to VAR Ct ( $n = 9$ ), and therefore  $n = 81$  for each RNA transcriptional activator. The means of the pooled fold difference values for each RNA transcriptional activator were compared by a one-way analysis of variance followed by Tukey's pairwise comparison (95% confidence interval). Individual pairs of data were compared by  $t$  test.

## ■ ASSOCIATED CONTENT

### ● Supporting Information

Supporting figures and tables. This material is available free of charge via the Internet at <http://pubs.acs.org>.

## ■ AUTHOR INFORMATION

### Corresponding Author

\*Tel: +1-513-558-5605. Fax: +1-513-558-3028. E-mail: ryan.kramer@wpafb.af.mil.

### Notes

The authors declare no competing financial interest.

## ■ ACKNOWLEDGMENTS

We thank Dr. K. Greis at the University of Cincinnati Cancer and Cell Biology Proteomics Core Facility and Dr. N. Kelley-Loughnane, M. Davidson, A. Stapleton, G. Sudberry, and J. Wright at 711th Human Performance Wing for their assistance. This work is funded by the Bio-X STT, Air Force Research Laboratory.

## ■ REFERENCES

- (1) Storz, G. (2002) An expanding universe of noncoding RNAs. *Science* 296, 1260–1263.
- (2) Storz, G., Altuvia, S., and Wassarman, K. M. (2005) An abundance of RNA regulators. *Annu. Rev. Biochem.* 74, 199–217.
- (3) Mattick, J. S. (2004) RNA regulation: a new genetics? *Nat. Rev. Genet.* 5, 316–323.
- (4) Waters, L. S., and Storz, G. (2009) Regulatory RNAs in bacteria. *Cell* 136, 615–628.
- (5) Wassarman, K. M., and Storz, G. (2000) 6S RNA regulates E. coli RNA polymerase activity. *Cell* 101, 613–623.
- (6) Novick, R. P., Iordanescu, S., Projan, S. J., Kornblum, J., and Edelman, I. (1989) pT181 plasmid replication is regulated by a countertranscript-driven transcriptional attenuator. *Cell* 59, 395–404.
- (7) Storz, G., Opdyke, J. A., and Wassarman, K. M. (2006) Regulating bacterial transcription with small RNAs. *Cold Spring Harbor Symp. Quant. Biol.* 71, 269–273.
- (8) Buskirk, A. R., Kehayova, P. D., Landrigan, A., and Liu, D. R. (2003) In vivo evolution of an RNA-based transcriptional activator. *Chem. Biol.* 10, 533–540.
- (9) Saha, S., Ansari, A. Z., Jarell, K. A., and Ptashne, M. (2003) RNA sequences that work as transcriptional activating regions. *Nucleic Acids Res.* 31, 1565–1570.
- (10) Wang, S., Shepard, J. R. E., and Shi, H. (2010) An RNA-based transcription activator derived from an inhibitory aptamer. *Nucleic Acids Res.* 38, 2378–2386.
- (11) Windbichler, N., von Pelchrzim, F., Mayer, O., Csaszar, E., and Schroeder, R. (2008) Isolation of small RNA-binding proteins from E. coli. *RNA Biol.* 5, 1–11.
- (12) Culler, S. J., Hoff, K. G., and Smolke, C. D. (2010) Reprogramming cellular behavior with RNA controllers responsive to endogenous proteins. *Science* 330, 1251–1255.
- (13) Liu, C. C., and Arkin, A. P. (2010) The case for RNA. *Science* 330, 1185–1186.
- (14) Isaacs, F. J., Dwyer, D. J., Ding, C., Pervouchine, D. D., Cantor, C. R., and Collins, J. J. (2004) Engineered riboregulators enable post-transcriptional control of gene expression. *Nat. Biotechnol.* 22, 841–847.
- (15) Harbaugh, S. V., Davidson, M. E., Chushak, Y. G., Kelley-Loughnane, N., and Stone, M. O. (2008) Riboswitch-based sensor in low optical background. *Proc. SPIE* 7040, 70400C.
- (16) Topp, S., and Gallivan, J. P. (2010) Emerging applications of riboswitches in chemical biology. *ACS Chem. Biol.* 5, 139–148.
- (17) Hunsicker, A., Steber, M., Mayer, G., Meitert, J., Klotzsche, M., Blind, M., Hillen, W., Berens, C., and Suess, B. (2009) An RNA aptamer that induces transcription. *Chem. Biol.* 16, 173–180.
- (18) Lucks, B. J., Qi, L., Mutalik, V. K., Wang, D., and Arkin, A. P. (2011) Versatile RNA-sensing transcriptional regulators for engineering genetic networks. *Proc. Nat. Acad. Sci. U.S.A.* 108, 8617–8622.
- (19) Bernstein, D. S., Buter, N., Stumpf, C., and Wickens, M. (2002) Analyzing mRNA-protein complexes using a yeast three-hybrid system. *Methods* 26, 123–141.
- (20) Zuker, M. (2003) Mfold web server for nucleic acid folding and hybridization prediction. *Nucleic Acids Res.* 31, 3406–3415.
- (21) Altschul, S. F., Gish, W., Miller, W., Myers, E. W., and Lipman, D. J. (1990) Basic local alignment search tool. *J. Mol. Biol.* 215, 403–410.
- (22) Ptashne, M., and Gann, A. (1997) Transcriptional activation by recruitment. *Nature* 386, 569–577.
- (23) Bushman, F. D., Shang, C., and Ptashne, M. (1989) One glutamic acid residue plays a key role in the activation function of lambda repressor. *Cell* 58, 1163–1171.
- (24) Busby, S., and Ebright, R. H. (1994) Promoter structure, promoter recognition, and transcription activation in prokaryotes. *Cell* 79, 743–746.
- (25) Buskirk, A. R., Landrigan, A., and Liu, D. R. (2004) Engineering a ligand-dependent RNA transcriptional activator. *Chem. Biol.* 11, 1157–1163.
- (26) Thompson, J. D., Gibson, T. J., Plewniak, F., Jeanmougin, F., and Higgins, D. G. (1997) The CLUSTAL\_X windows interface: flexible strategies for multiple sequence alignment aided by quality analysis tools. *Nucleic Acids Res.* 25, 4876–4882.
- (27) Livak, K. J., and Schmittgen, T. D. (2001) Analysis of relative gene expression data using real-time quantitative PCR and the  $2^{-\Delta\Delta\text{Ct}}$  method. *Methods* 25, 402–408.